Agricultural and Forest Meteorology 346 (2024) 109871

Contents lists available at ScienceDirect

Agricultural and Forest Meteorology

journal homepage: www.elsevier.com/locate/agrformet

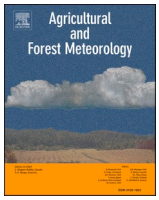

The intra-annual rhythm of *Pinus sylvestris* growth-climate responses under a warming climate at its southern distribution limits

Junxia Li [a,b], Yuting Jin [b], Ying Zhao [b], Tsun Fung Au [c,d], Yucheng Wang [a,e,f,*,1], Zhenju Chen [b,g,h,i,*,1]

[a] College of Horticultural, Shenyang Agricultural University, Shenyang 110866, China
[b] Tree-Ring Laboratory/Research Station of Liaohe-River Plain Forest Ecosystem CEN, College of Forestry, Shenyang Agricultural University, Shenyang 110866, China
[c] Institute for Global Change Biology, School for Environment and Sustainability, University of Michigan, Ann Arbor, MI, United States
[d] Department of Ecology and Evolutionary Biology, University of Michigan, Ann Arbor, MI, United States
[e] College of Forestry, Shenyang Agricultural University, Shenyang 110866, China
[f] Key Laboratory of Forest Tree Genetics, Breeding and Cultivation of Liaoning Province, Shenyang 110866, China
[g] Qingyuan Forest CERN, Chinese Academy of Sciences, Shenyang 110164, China
[h] Key Laboratory of Desert and Desertification, Chinese Academy of Sciences, Lanzhou 730000, China
[i] National Research Station of Changbai Forest Ecosystem, Er'daobaihe 133613, China

ARTICLE INFO

Keywords:
Response rhythm
Intra-annual
Temperature
Threshold
Xylogenesis

ABSTRACT

Warming climate has posed a pressing threat on boreal forests and an improved understanding of the intra-annual pattern of climatic influences on the tree growth can help interpret the response of boreal forest to climate change. Here, we systematically examined the growth-climate relationship, cambium phenology, and xylem cell dynamics of *Pinus sylvestris* (*PS*) to disentangle its intra-annual growth rhythm to external drivers and internal physiological process at its southern distribution limits across Eurasia. We showed the intra-annual rhythm of *PS* to temperature and precipitation is anti-phase and synchronous at its southern limits. Temperature had both promoting and inhibiting effects on *PS* growth over growing season where the growth-temperature response gradually changed from positive in winter-early spring to negative in late spring-summer, and then returned to positive in autumn. Precipitation enhanced *PS* growth in late spring-summer. Temperature dominated the intra-annual growth-climate response rhythm, and the response shifted to negative when temperature reached 13.72 °C in spring-summer and shifted to positive when temperature reached 17.41 °C in summer-autumn in Shenyang, respectively. A high water demand for the rapid earlywood cell formation in spring-summer and heat requirement for cambial cell division in summer-autumn caused the shifts in growth-temperature response, respectively. Climatic warming advances and prolongs the time of summer water availability that limits *PS* growth at its southern distribution limits and thus warming climate may pose a greater threat to the southern population of *PS*.

1. Introduction

Boreal forests occupy approximately 11 % of the earth's surface (Safford and Vallejo, 2019) and hold ca. 20 % of the global carbon sinks (Pan et al., 2011), which play critical roles in regulating global carbon and water cycles (Richardson et al., 2013). Among them, wood formation takes up around 15 % of the anthropogenic CO_2 emissions per year (Huang et al., 2020). However, seasonal warming temperatures compounded with reduced moisture availability have caused a decline in tree growth (Lindner et al., 2014), productivity (Ciais et al., 2005), resilience from disturbance (Gilliam, 2016), and even triggered forest mortality (Allen et al., 2010; Schaphoff et al., 2016). Thus, an improved

Abbreviations: PS, *Pinus sylvestris*; EW, Earlywood; LW, Latewood; TR, Total ring; Tmax, Mean maximum temperature; T, Mean temperature; Tmin, Mean minimum temperature; P, Precipitation; RH, Relative humidity; SPEI, Standardized precipitation evapotranspiration index; CZ, Cambial zone cell; EN, Enlargement cell; WT, Wall thickening and lignifying cell; MT, Mature cell; TC, The total xylem cell number.

* Corresponding authors at: College of Forestry, Shenyang Agricultural University, Shenyang 110866, China
E-mail addresses: wangyucheng@ms.xjb.ac.cn (Y. Wang), chenzhenju@syau.edu.cn (Z. Chen).

[1] Both authors as co-correspondence contributed equally to this work.

https://doi.org/10.1016/j.agrformet.2023.109871
Received 1 March 2023; Received in revised form 19 December 2023; Accepted 20 December 2023

understanding of the intra-annual pattern of climate influences on the tree growth of common species is necessary for interpreting the response of boreal forest growth to climate change.

Many relevant studies have found that warmer winter and early spring temperatures were positively related to boreal conifer growth (Babst et al., 2019; Harvey et al., 2020) and the lagged effects such as earlier snow melt and soil warming were thought to lengthen the growing season and promoted early tree growth (D'Orangeville et al., 2016), while high summer temperatures enhanced evapotranspiration and thus induced drought stress and constrained tree growth (Waszak et al., 2021; Kuznetsova and Solomina, 2022). However, these studies mainly focused on the direction and magnitude of growth-climate response at monthly and seasonal scales but neglected to investigate the intra-annual response mechanism, including response trajectories, thresholds, and intrinsic processes.

Pinus sylvestris (Scots pine, hereafter *PS*) is one of the common species in the boreal forests with many subspecies and varieties (Durrant et al., 2016). *PS* is widely distributed in middle-high latitudes across Eurasia, from Europe to Russian Far East and Northeast China (https://www.euforgen.org/species/pinus-sylvestris/, Fig. 1a). The climate in *PS* distribution area ranges from the Mediterranean climate (dry summer and mild winter) in the west to the temperate monsoon climate (wet summer and cold winter) in the east across a wide hydrothermal gradient. The response of *PS* growth to climate change could directly affect the structure and function of boreal forests. Many studies employed traditional dendrochronological methods to investigate the intra-annual response of *PS* growth to climate change (Fig. 1a). These studies mainly analyzed the correlation between tree growth and climate variables, and there appears to be an intra-annual rhythm in *PS* growth-climate relationship in a growing year in different regions of the southern distribution range. For example, Martin-Benito et al. (2013) found that previous-year or early-season conditions affected *PS* earlywood features, whereas latewood was more responsive to summer climate in east-central Spain. In western Hungary, summer precipitation and late winter-early spring temperature had a positive influence on the *PS* tree-ring width (Misi and Náfrádi, 2017). Bozkurt et al. (2021) found

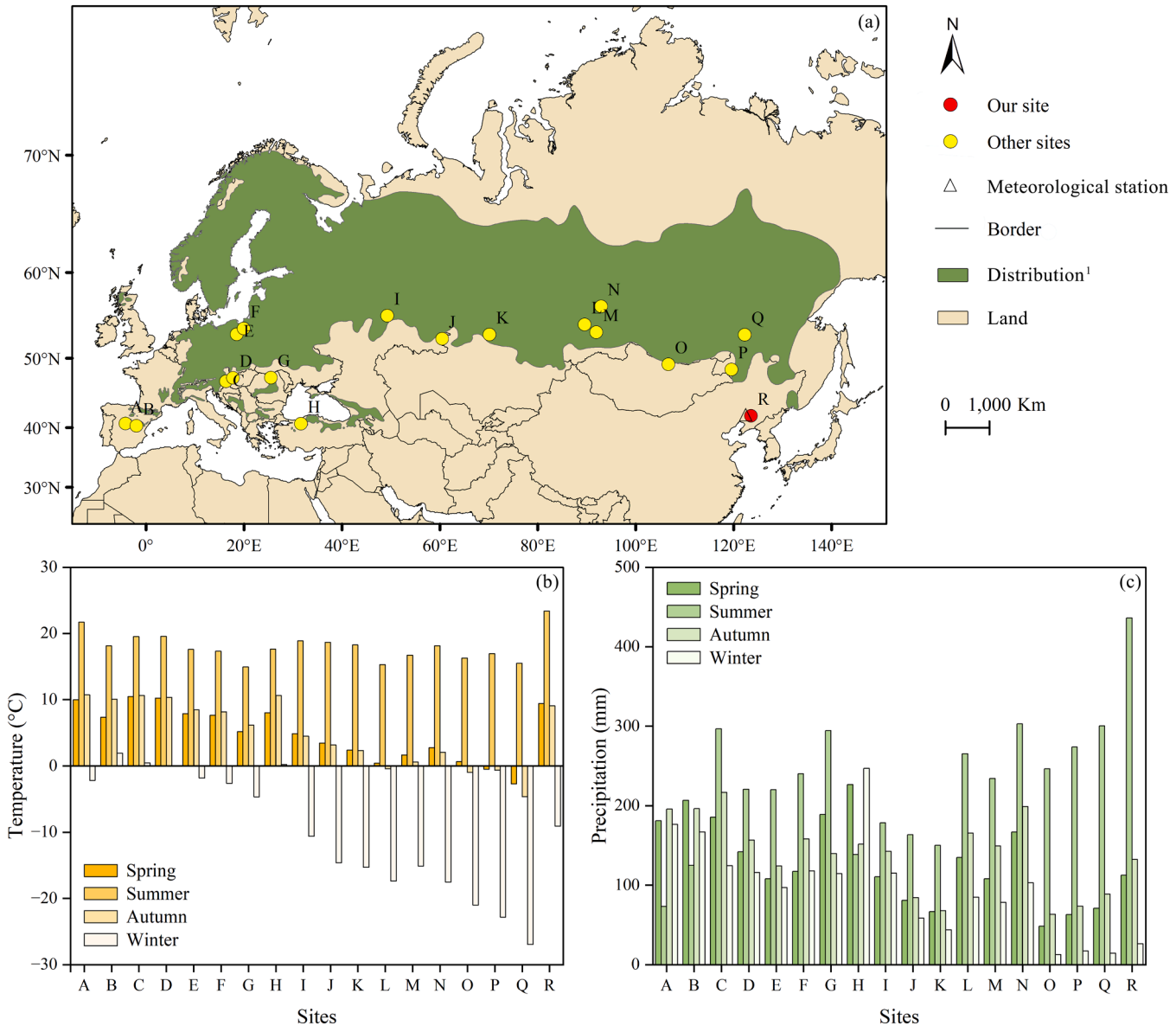

Fig. 1. The tree-ring sites at the southern limits of *PS* distribution[1] throughout Eurasia (a) and their seasonal climate during 1951–2020 (b, c). A-R, 18 *PS* sampling sites, arranged from west to east (Table S1). A-Q, other's sites arranged from west to east; R, our site in Shenyang. 1, the species range was from https://www.euforgen.org/species/pinus-sylvestris/. Spring, March-May; summer, June-August; autumn, September-November; winter, December-February.

that early spring temperature and late spring-early summer precipitation were the major drivers of *PS* growth in Turkey. Arzac et al. (2021) found that the negative effect of summer temperature and the positive effect of relative humidity on *PS* growth were enhanced in Krasnoyarsk Krai of Russia. Kuznetsova and Solomina (2022) also found a negative relationship between temperature and *PS* ring width in the Middle Volga region over the current growing season. However, these studies did not disentangle the intra-annual rhythm of *PS* growth-climate response. Thus, the threshold and the physiological mechanism of intra-annual response variation for *PS* were still unclear and necessitate a thorough investigation.

A prerequisite for quantifying the impacts of climate change is to identify the threshold of climate impacts on forests. Improved understanding on the response threshold has a very important theoretical and practical significance for examining the magnitude and extent of climate change impacts. This allows us to minimize damage and even maximize the opportunity of climate change adaptation before reaching the threshold (Huang et al., 2022). The inter-annual and spatial thresholds of climate influences on tree radial growth were identified in some previous studies using the dendrochronological methods. For instance, at the inter-annual scale, the persistent increase in July–August temperature over time but temperature above 11.3°C had a negative effect on tree-ring width (D'Arrigo et al., 2004), while the March-April temperature threshold for *PS* in Turkey was 7°C where trees growth decreased beyond this temperature (Bozkurt et al., 2021). At the spatial scale, the tree-ring widths increased as May–August temperatures warm, but only up to 11–12°C, from western tree line along the Bering Sea coast to the continental interior of the species range (Beck et al., 2011). Bai et al. (2019) inferred that the mean annual temperature threshold of response shift of *Larix gmelinii* to temperature and precipitation along altitude gradient was ca. –4°C and ca. –5°C, respectively, in northeast China. However, the intra-annual threshold of tree growth-climate response had less attention in dendrochronological studies. The intra-annual threshold was critical for disentangling the rhythm of tree growth-climate response and predicting the future climate impact pattern. In addition, it was difficult to understand the formation mechanism of these thresholds of growth-climate response merely by the dendrochronological methods.

Repeated monitoring cambial phenology and xylem dynamics using the micro-sampling approach is ideal for understanding the eco-physiological processes of tree responding to intra-annual climate change (Rossi et al., 2006a; Michelot et al., 2012). Radial growth is a complex process and involves cell division in the cambial zone, followed by cell enlargement, secondary wall thickening and lignification (Rossi et al., 2006b). Studies of xylem growth in boreal forests using this approach revealed that there was an annual cyclic pattern in cambium activities and xylem formation (Deslauriers et al., 2003; Huang et al., 2018; Rossi et al., 2006). For example, the intra-annual pattern of *PS* growth was generally unimodal at the European sites with the peak of growth in spring–summer (Camarero et al., 2010; Cuny et al., 2012; Oberhuber et al., 2014, 2021; Swidrak et al., 2014). Moreover, the xylogenesis phases of *PS* at different sites followed a common pattern during the growing season (Martínez del Castillo et al., 2016). The cell enlarging and wall-thickening curves were bell-shaped, while the cell maturation curve was sigmoid-shaped (Gruber et al., 2010; Swidrak et al., 2014; Martínez del Castillo et al., 2016). Furthermore, cambial activity of *PS* adopted an 'extensive strategy' with long durations but low growth rates compared with other conifers (Cuny et al., 2012). The duration of xylem growth for *PS* mostly lasted 2–7 months at the European sites (Gruber et al., 2010; Michelot et al., 2012; Cuny et al., 2012; Martínez del Castillo et al., 2016). The cyclical pattern of xylem growth was a response to seasonal climate change (Rossi et al., 2008; Huang et al., 2014; Cuny et al., 2015). For example, spring (April–May) temperatures were the main factors for regulating cambium activities and xylem formation of conifers in mid-high latitudes of the northern hemisphere (Rossi et al., 2016). Cessation of cambial activity in autumn was affected by temperature in cold regions (Rossi et al., 2016) and water availability in dry regions (Swidrak et al., 2014). A precise assessment of xylem dynamics is therefore crucial for disentangling intra-annual tree growth response to climate change. Monitoring wood formation at the limits of the species' distribution is especially relevant, since these trees are most sensitive to climatic factors (Gruber et al., 2010; Martínez del Castillo et al., 2016).

In this study, we incorporated existing and new correlation results between climate variables and tree growth of *PS* at its southern distribution limits across Eurasia to assess the intra-annual pattern of growth–climate relationships at a broad scale and explore the reason of response shift. We further monitored xylogenesis of *PS* using micro-coring to identify the onset, dynamics and end of intra-annual growth at the southern limit site. The aims of our study were: (a) to identify the broad-scale intra-annual rhythm of *PS* growth-climate responses at its southern distribution limits; (b) to determine the dominant climate factor and its threshold influencing intra-annual response shift; (c) to reveal the formation mechanism of the intra-annual rhythm.

2. Materials and methods

2.1. Study area

Our study spanned a wide environmental gradient, mainly encompassing the boreal forests across Eurasia (Fig. 1a). *PS* is a pioneer species, cold and drought tolerant and can grow in diverse climatic environments (Durrant et al., 2016). We leveraged 17 former studies of *PS* tree-ring data to identify the intra-annual variation of growth-climate responses of *PS* at its southern distribution limits (Agafonov et al., 2021; Arzac et al., 2021; Bogino et al., 2009; Bozkurt et al., 2021; Kolář et al., 2020; Kopabayeva et al., 2017; Kuznetsova and Solomina, 2022; Li et al., 2017; Martin-Benito et al., 2013; Misi and Náfrádi, 2017; Misi et al., 2019; Nagavciuc et al., 2019; Tabakova et al., 2020; Waszak et al., 2021) (Fig. 1a, A-Q). In total, 753 trees (> 1196 cores) were collected in these studies (Table S1). The sampling sites we selected were relatively evenly-distributed with different climatic environments, which can improve the regional representativeness and reduce bias. These study sites were distributed from 40 °N to 57 °N and 4 °W to 125 °E across a wide climatic gradient in annual mean temperatures (−4.7 to 10.3°C, 1951–2020) and annual precipitations (328 to 823 mm) (Fig. 1a). Both maritime and continental weather patterns modulate climate across the study region. There were diverse climatic types in the *PS* distribution area, such as Mediterranean climate (site A, B, H, etc.), temperate continental climate (site I, J, K, etc.), temperate monsoon climate (site Q, P, R, etc.). Seasonal climate also varied among these sites, with the greatest differences in winter temperatures (the lowest −26.9°C vs the highest 1.9°C) and summer precipitation (the lowest 73 mm vs the highest 436 mm) (Fig. 1b, c).

We also investigated a *PS* population in Shenyang, Northeast China (Fig. 1a, R), which was located in the southern margin of cold-temperate coniferous forest. The landform was mainly plain with relatively low altitude (< 100 m, Fig. 1a). The soil was mainly brown and dark-brown forest soil. *PS* was one of the main tree species in this area, accompanied by *Pinus tabuliformis, Quercus mongolica*, and *Q. wutaishansea.*

This area was characterized by a warm temperate monsoon climate with an average of 8.2°C in annual mean temperature in 1951–2020 (Shenyang meteorological station). From March to October, the mean air temperature was above 0°C (Fig. S1a). This study area belonged to the humid climate with an average annual precipitation of 707 mm. Over 60 % annual precipitation was concentrated in the monsoon season (June-August) (Fig. S1a). The snow cover decreased from 65 % to nearly 0 in January-April and increased from 0 to 52 % in October-December (Fig. S1b). From 1952 to 2020, mean temperatures of previous November–current April, May–August and September–October all significantly increased ($p < 0.01$, Fig. S2a). The total precipitation of September–October decreased significantly ($p < 0.05$, Fig. S2b). Mean

temperature and total precipitation of September-October displayed a significantly opposite decadal trend ($p < 0.01$) during 1951–2020 in this area (Fig. S3), indicating that increased precipitation in autumn could cool down the air.

2.2. Meteorological data

Daily and monthly climate data including mean maximum temperature (Tmax), mean temperature (T), mean minimum temperature (Tmin), and precipitation (P) from 1951 to 2020 were available at the closest Shenyang meteorological station (41.73 °N, 123.52 °E, 490 m) (Fig. 1a), which was obtained from the National Meteorological Information Center (http://data.cma.cn/). The 1-month Standardized precipitation evapotranspiration index (SPEI, 1951–2018) and snow cover extent (1967–2020) for our site were obtained from KNMI Climate Explorer (http://climexp.knmi.nl). The monthly mean temperature and precipitation for 17 other sites were also obtained from KNMI Climate Explorer.

2.3. Tree-ring sampling and chronology developing

Tree-ring cores of *PS* were taken from Tianzhushan Mountain in Shenyang, China (Fig. 1a) in late November 2020. We sampled 23 healthy, upright trees using an increment borer at breast height, with two cores per each tree. Based on the standard dendrochronological procedure (Cook and Kairiukstis, 1990; Stokes and Smiley, 1968), all cores (46 cores) were fixed, air-dried and polished with sandpapers of grit size from 120 to 1000 to make tree-ring boundary visible and discernable.

The earlywood (EW), latewood (LW), and total ring (TR) widths chronologies of all 46 tree-ring series from 23 trees were developed by a LINTAB 5 tree-ring width measuring system (RINNTECH, Heidelberg, Germany) with a precision of 0.01 mm. The EW and LW measurements were made at the distinct boundary between EW and LW, whereas for gradual EW–LW transition, the measurement was made at the middle of the transition (Stahle et al., 2009). For false ring, the measurement was made at the first onset of lumen contraction (Stahle et al., 2009). There were 53 false rings in 46 cores. The cross-dating and measurement accuracy was checked statistically with COFECHA software (Holmes, 1983).

To minimize the influence of non-climatic factors on tree growth, the raw measurements of EW, LW, and TR were detrended and converted to tree-ring indices using the Friedman curve-fitting method (−5) with an alpha value of 7 (variable span tweeter sensitivity) in the ARSTAN software (Cook and Kairiukstis, 1990). The EW, LW, and TR standard chronologies were developed by the robust bi-weight mean to reduce the effect of extreme indices on calculating average values (Fig. S4). The lengths of the EW, LW and TR chronologies were 69 years (1952–2020), and their reliable periods were 1959–2020 with expressed population signal (EPS) greater than 0.85 (Wigley et al., 1984). The correlations between the three chronologies were significant (Table S2, $p < 0.01$).

The high series intercorrelation (0.43–0.59) and signal-to-noise ratio (21.90–31.33) indicated that chronologies contained common climatic signal (Table S3). The mean sensitivity (0.20–0.32) and standard deviation (SD, 0.21–0.32) were acceptable. The EPS values (>0.95) of all three chronologies were above the usual threshold of 0.85, indicating their good quality.

2.4. Dendrochronological statistics analysis

We examined the growth–climate relationships between the EW, LW, and TR chronologies and monthly climate variables (Tmax, T, Tmin, P and SPEI) by Pearson's correlation during the common period 1959–2020 with the EPS value over 0.85. We selected the months from November of a previous year to October of a current year as a growing year to study the intra-annual variation of growth–climate relationship. To minimize the autocorrelation effects, we used the first-order difference variables of EW, LW, TR chronologies and climate variables in the correlation analysis. We also defined seasonal climate variables based on monthly correlation results (positive or negative) with temperatures (Tmax, T, Tmin), as follows: early season (previous November to current April), middle season (current May to August) and late season (current September to October). We used linear regression to simulate the variation of TR-climate correlation along monthly climate gradient to identify the dominant factor of the intra-annual variation of growth-climate relationship. We integrated our correlation results with the previous 17 studies of *PS* to explore the common growth pattern at monthly interval. The correlation coefficients of all 18 sites were averaged to reflect the intra-annual growth-climate relationship of *PS* at its southern distribution limits. Then, we calculated the correlation coefficient of the averaged growth-temperature correlation series and the averaged growth-precipitation correlation series to reflect the relationship of the regional growth-temperature response and growth-precipitation response.

Given that climate data at the dekad scale allows a more precise examination of intra-annual growth-climate relationship (Qi et al., 2022), we divided each month into three phases (I: the first ten days of a month; II: the second ten days of a month; III: the rest days of a month). Average air temperature and the sums of precipitation for the three phases of a month were calculated using daily climate data in Shenyang. We calculated the correlation coefficients between all tree growth parameters (EW, LW, and TR) and climate variables (Tmax, T, Tmin, and P) at ten-day interval (dekad scale) using the first-order difference series. A linear model was used to quantify the potential effects of hydrothermal change on growth-climate response in different phases and identify the thresholds for the adaptability of pine's populations under changing hydrothermal conditions. Since EW and LW formed in different seasons (Rossi et al., 2006), our linear models were estimated for hydrothermal variables and EW-climate responses in early-middle season, and for LW-climate responses in middle-late season. Meanwhile, temperature thresholds for growth-temperature response were determined in both early-middle and middle-late seasons, respectively. We then used the temperature thresholds to obtain the mean occurrence dates during the past 70 years. The start date, end date, and duration of water availability limiting growth in a year were also determined from 1951 to 2020.

2.5. Xylem growth monitoring and analysis

We investigated the physiological process in terms of cambium and xylem monitoring in Shenyang in 2019 because the monthly climate conditions in 2019 ranged within the average of the observational records. Micro-cores of six trees were sampled on the south side of the trunk of *PS* at the same site using the Trephor tool (Rossi et al., 2006b) (Table S4). We started sampling on March 3, 2019 and collected every Sunday until November 10, 2019 (Table S5). These individual trees were healthy, canopy-dominant, and similar in stem diameter at breast height (ranging from 21.7 to 33.5 cm) and age (~40 years). The micro-cores of each tree containing phloem, cambium, and the last formed xylem growth ring were collected at breast height following a Z pattern. Then, micro-cores were stored in formaldehyde ethanol-acetic acid fixative solution, and cut by a sliding ultrathin microtome (type GSL, Switzerland) with a 2 mm thickness blade to obtain micro-core sections that were 8–16 μm thick. The micro-core sections were then stained, dehydrated, and sealed to create permanent slides. The micro-core sections were stained with safranin and fast green solutions, and observed with an OLYMPUS light microscope under a bright field and polarized light at 100–400 × magnification, to discriminate and count the number of the cambial zone (CZ), enlargement (EN), wall-thickening (WT), and mature cells (MT) along three radial files (Deslauriers et al., 2003). The xylem cell numbers were standardized by the total cell number in the tree-ring of the previous year (Deslauriers et al., 2003;

Rossi et al., 2003) and then cell counts were averaged by trees.

Cambial zone cells (CZ, Fig. S5) were characterized as small radial lumen diameter and thin cell walls that were stained green. Enlargement cells (EN, Fig. S5) were also stained green with a thin cell wall but with a radial diameter that was twice bigger than that of the cambial cells (Lupi et al., 2010). Wall thickening and lignifying cells (WT, Fig. S5) were stained green or light red, depending on the progress of the lignification (Gričar et al., 2006). Polarized light helped to discriminate between enlarging cells and bi-refringent wall-thickening cells. Mature cells (MT, Fig. S5) had lignified walls without protoplasts were completely red when stained. The total xylem cell (TC) number for each sample was determined by the number of cells undergoing enlargement, wall thickening, and mature stage (Deslauriers et al., 2003).

The EW cell number was equal to the sum of EW cells undergoing enlargement, wall thickening, and mature. The appearance of latewood cells, characterized by reduced radial lumen diameter and thickened cell walls, was also recorded to define the transition between EW and LW during the summer. Previous definitions of LW were based on mature LW cells (complete wall-thickening and lignification), and a tracheid was considered LW when its radial diameter was less than twice cell-wall thickness (Denne, 1988). In fact, LW growth started when enlarging LW cells appeared. Thus, the onset time of LW growth was later than the actual date if using the previous distinction criteria. In order to determine the LW formation time accurately, we defined LW cell formation as when the radial diameter of the newly produced enlarging cells in summer is less than half radial diameter of the previous cells (Fig. 2a) with cell wall thickening and lignifying in the later period (Fig. 2b, c). The LW cell number was equal to the sum of LW cells undergoing enlargement, wall thickening, and mature.

We identified phenology dates of xylem growth based on the direct observations of cell differentiation, including the onset of EN, WT and MT; end of EN and WT; and duration of EN, WT, MT and xylem growth. The onsets of wood production and xylem growth in spring were considered when as at least one horizontal row of EN cells was observed. In autumn, wood production ended when no further EN cells were observed, and xylem growth ended when no further WT cells were observed. The duration of wood production was defined as the period between the onset and end of EN (Rossi et al., 2014). The duration of xylem growth was calculated as the period from the onset of EN to the end of WT (Rossi et al., 2006b). In addition, the duration of EW formation was defined from the onset of the first enlargement cell in spring to the end of the last wall thickening and lignification EW cell in summer. The duration of LW growth was from the onset of the first enlargement LW cell in summer to the end of the last wall thickening and lignification cell in autumn. We compared the synchronous time series of cambium phenology, xylem cell dynamics, and growth-climate response of *PS* to understand the physiological process of intra-annual rhythm of growth-climate response.

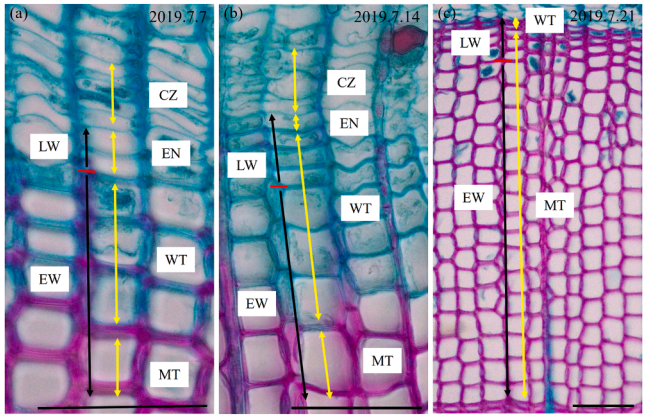

Fig. 2. Dynamics of latewood (LW) formation of *PS* in 2019. (a), on 7 July 2019, new enlarging LW cell was observed; (b), on 14 July, wall-thickening LW cell was observed; (c), on 21 July, mature LW cells were observed. EW, earlywood; CZ, cambial zone cells; EN, enlargement cells; WT, wall-thickening and lignifying cells; MT, mature cells. The yellow arrows represent cells at different stages. The black arrows represent EW and LW cells. The red horizontal lines represent the boundaries of EW and LW. The black horizontal lines represent the scale bar (100um).

To investigate the intra-annual dynamics of xylem growth, the EW (LW) cell number was fitted with the Gompertz function (Rossi et al., 2003) with the following equation:

$$y = A\exp\left[-e^{(\beta-kt)}\right]$$

where y was the weekly cumulative sum of EW (LW) cells, A was the upper asymptote given by the total number of EW (LW) cells, β was the x-axis placement parameter, κ was the rate of change parameter, and t was the day of the year. The maximum rate of EW (LW) cell production was computed as $\kappa A/e$ and the corresponding date of the inflection point of EW (LW) was calculated as β/κ (Rathgeber et al., 2011). Model parameters were estimated using the Origin software package (OriginLab Corporation, USA). The daily growth rate of EW (LW) was obtained by taking the first derivative for the Gompertz curve and monthly growth percentage for EW (LW) cells were calculated based on the simulated cell number.

Temperature thresholds for xylogenesis were calculated using a logistic regression based on the binary responses (non-active = '0', active = '1') of xylogenic activity for each tree (Rossi et al., 2007). The logistic regression model was as follow:

$$\mathrm{Logit}(\pi_x) = \ln\left(\frac{\pi_x}{1-\pi_x}\right) = \beta_0 + \beta_1 x_j$$

where π_x was the probability of xylogenesis being active for a given temperature x, x_j was the temperature on a given day j, and β_0 and β_1 were intercept and slope of the logit regression respectively (Rossi et al., 2007). Temperature thresholds (x) were calculated when the probability of xylogenesis being active was 0.5, thus when $\mathrm{logit}(\pi_x) = 0$ and therefore, $x = -\beta_0/\beta_1$. For each tree, temperature thresholds of onset of xylem growth, end of wood production and end of xylem growth were computed based on the average temperature of ten days prior to each sampling date (including the current day). For each tree, the model was fitted with average temperature of ten days prior to each sampling date (including sampling date). The selection of ten-day interval was chosen because of the lagging effects of climate and keeping the same timescale with the previous correlation analysis. The thresholds of xylogenesis were compared with the temperature thresholds of growth-climate response to understand the internal reason of growth-climate response shift.

3. Results analysis

3.1. Comparison of intra-annual growth-climate response at the southern distribution limits

Although the strength and direction of correlations between *PS* growth and climate variables varied among the 18 sites (Fig. 3), we reported here a broadly dominant relationship between growth and climate at the southern distribution limits. The effect of temperature and precipitation on *PS* growth exhibited a synchronous but antagonistic pattern ($r = -0.79$, $p = 0.002$) within a growing year (Fig. 3).

Across these sites, *PS* growth was mostly and strongly positively related to mean temperature in February and March, and was mostly and strongly negatively related to mean temperature in May, June, and July (Fig. 3a). The mean growth-temperature correlation changed gradually from positive in November-April to negative in May-August and then to positive in September-October ("sine" type curve)

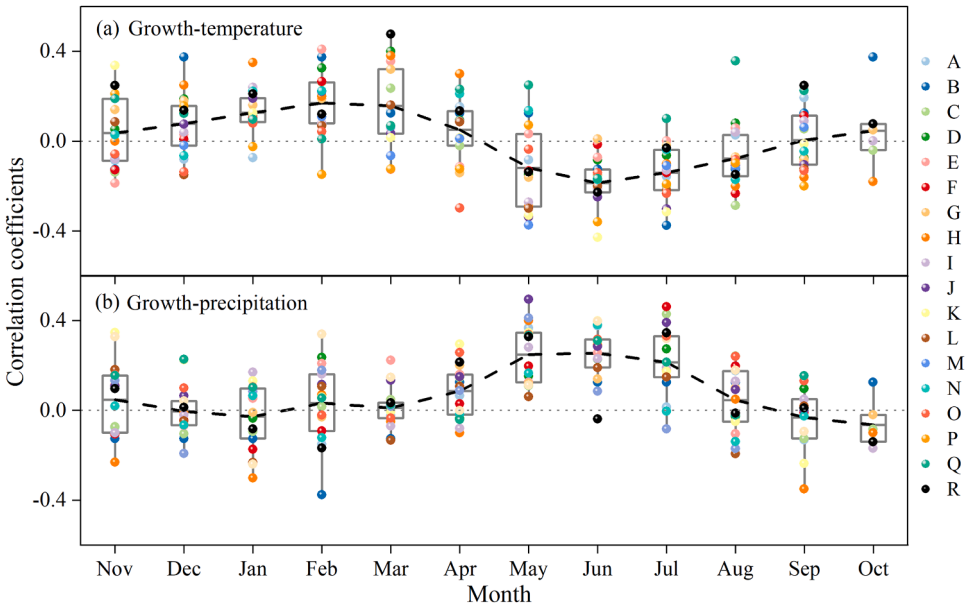

Fig. 3. The intra-annual variation of growth-climate responses of *PS* at the southern distribution limits in recent decades. (a), monthly mean air temperature; (b), monthly precipitation. The *PS* sampling sites (A–R, Table S1) are arranged in the ascending order of longitude. Box plots show mean, lower and upper quartiles (25 % and 75 %) of correlation coefficients of 18 sites. The black dashed lines represent the intra-annual variation of the mean value of correlation coefficients of 18 sites. The horizontal gray dashed lines represent the 0 value of correlation coefficients.

(Fig. 3a). *PS* growth was mostly and strongly positively related to precipitation in May, June, and July at many sites (Fig. 3b). The mean growth-precipitation response was weak in November–March and shifted to strongly positive in April-August and then changed to negative in September-October ("cosine" type curve) (Fig. 3b).

The growth-climate response in Shenyang was similar to the average growth-climate response of the rest 17 sites at the southern distribution limits ($r_T = 0.78$, $p < 0.01$; $r_P = 0.59$, $p < 0.05$) and, therefore, we conducted mechanistic examination on *PS* physiological responses in Shenyang to provide insight on *PS* tree growth under future warming climate.

3.2. Monthly and dekad climate–growth responses in shenyang

PS radial growth was enhanced by temperature in the early and late seasons, and by water availability in the middle season in Shenyang at both monthly (Fig. 4a) and ten-day (Fig. S6) intervals. The growth-temperature response shifted from strongly positive in early season to negative in middle season and then back to positive in late season (Fig. 4a). Conversely, the growth response to precipitation and SPEI changed from negative or positive in early season to strongly positive in middle season and then to negative in late season.

Most ring width index (EW, LW, and TR) had positive correlation with temperature variables in early and late seasons (Fig. 4a). Among them, March temperature had the strongest control on tree growth especially for EW ($r = 0.50 – 0.53$, $p < 0.01$). Negative correlation with temperature and positive correlation with precipitation and SPEI were found in middle season (Fig. 4a). Both Tmax and T in May and June inhibited the EW growth ($r = -0.25 – -0.32$, $p < 0.05$). Precipitation and SPEI in May had positive correlation with the EW growth, while that in July had positive effect on the LW growth ($p < 0.05$).

3.3. Effect of the hydrothermal variables on intra-annual growth-climate response

Temperature had the strongest impact on the intra-annual variation of growth-climate responses (R^2 ranging from 0.19 to 0.40, $p < 0.01$), especially growth-temperature response (Fig. 5). The correlations of TR-precipitation and TR-SPEI showed the significant increasing trends from negative to positive when temperature increases ($p < 0.01$) (Fig. 5a). The effect of hydrothermal variables on growth-precipitation response was weaker than that of growth-temperature response (Fig. S7).

In early-middle and middle-late seasons, temperature also showed a stronger effect on growth-climate response for EW and LW than precipitation (Fig. 6). EW(TR)-temperature correlation showed a significant shift ($p < 0.01$) from positive to negative when temperature increased and reached ca. 13.72°C (ca. 15.08°C) in early-middle season (Fig. 6a). LW(TR)-temperature correlation also showed a significant shift ($p < 0.05$) from negative to positive with temperature decreased and reached ca. 17.41°C (ca. 16.35°C) in middle-late season (Fig. 6b). We used the temperature thresholds of EW and LW for determining the occurrence dates of response shift in the following section.

Based on the temperature thresholds, from 1951 to 2020 the onset date of water availability-limited *PS* growth was significantly advanced (0.15 days/year), the end date was obviously delayed (0.10 days/year), the duration was significantly prolonged (0.20 days/year) (Fig. 7, $p < 0.01$) with the rapid seasonal temperature rise in Shenyang (Fig. S2a).

3.4. Intra-annual dynamics of tree-ring formation

The onset and end of tree-ring growth of *PS* occurred during the period of positive growth-temperature correlation (early and late phases), and the maximum rate occurred during the period of negative temperature-growth correlation and positive precipitation-growth correlation (middle phase) (Fig. 4; Fig. S8). The growth season of xylem lasted 179 days (from April 21 to October 17) in 2019 (Fig. 4b; Table S6). The CZ resumed activity in mid-March (when the CZ number exceeded 7), earlier than the onset of xylem growth (Fig. 4c). The EW and LW cells were produced within 91 and 103 days, respectively with 15 days overlapped (July 6 to July 21). The intra-annual dynamic for both EW and LW presented S-shaped curves (Fig. 4d). The growth rates of EW and LW reached their maximum in May and August, respectively, accounting for 22.5 % and 29.0 % of the total annual growth (Fig. 4e; Table S7).

In a growing season, the number of CZ, EN, and WT of *PS* showed a bimodal pattern (Fig. S8a, b, c) and the number of MC and TC were like

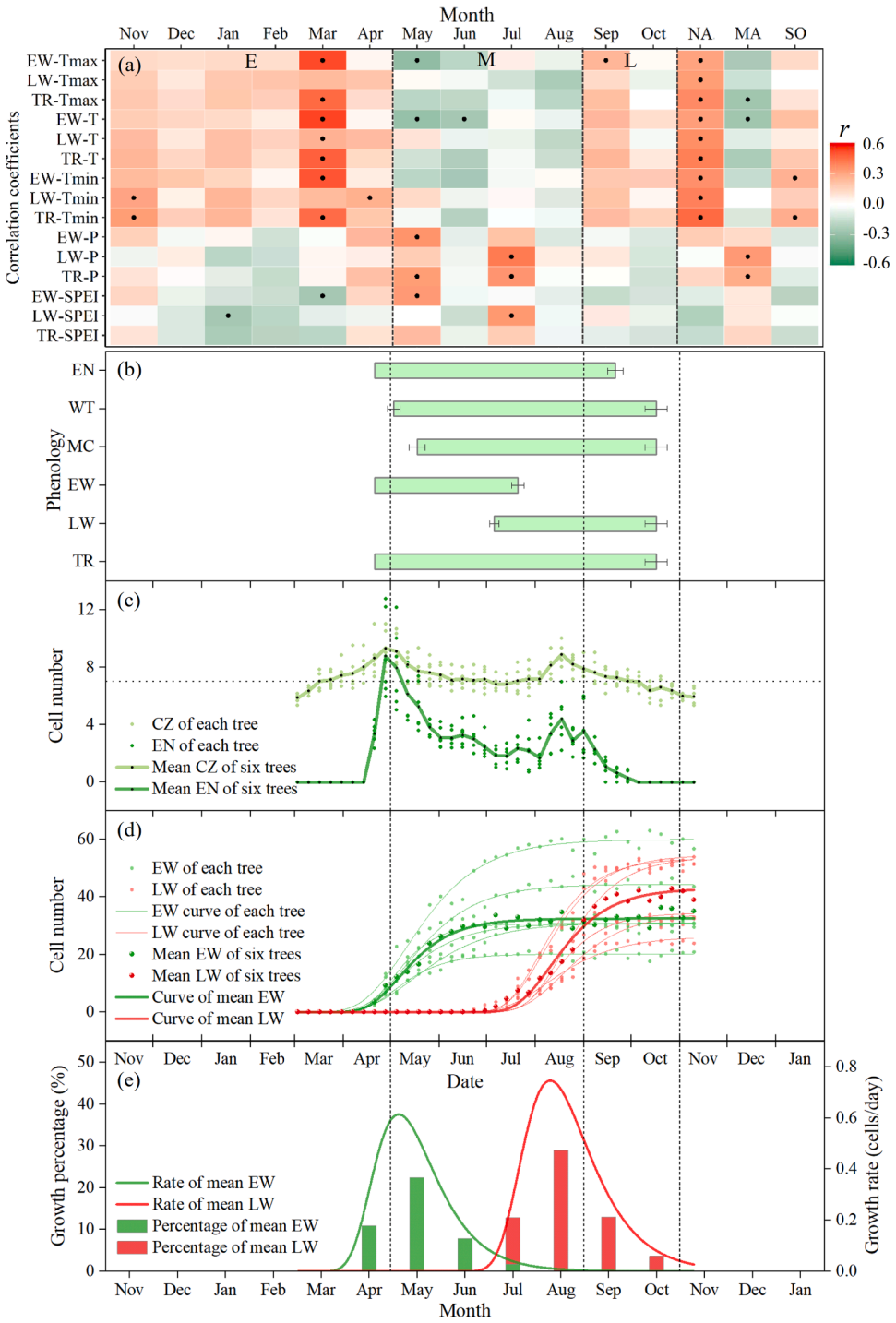

Fig. 4. The corresponding intra-annual dynamics of radial growth-climate correlation (a), xylem phenology (b), cambium activity (c) and xylem cell growth (d, e) for *PS* during early season (E: November–April, NA), middle season (M: May–August, MA) and late season (L: September–October, SO). The vertical dashed lines distinguish between early, middle and late seasons. (a): correlation coefficients between tree-ring width in terms of earlywood (EW), latewood (LW), and total ring (TR) and monthly/seasonal climate variables in a growing year during 1959–2020 (SPEI, 1959–2018). Black dots indicate significance at the 0.05 level. (b): phenological date of *PS* radial growth in terms of enlargement (EN), wall-thickening (WT), mature cells (MC), EW, LW, and TR in 2019. The phenological dates of EN and TR indicate the dates of wood production and xylem growth, respectively. Horizontal bars show the average onset date, end date and duration of each seasons and error bars indicate the standard deviation among trees. (c): intra-annual dynamics of cambial zone (CZ) and EN cells of *PS* in 2019. The horizontal gray dotted line represents the 7 value of cell number. (d): intra-annual dynamics of EW and LW growth of *PS* modeled by the Gompertz function (for parameters, see Table S7). (e): monthly growth percentage and daily growth rate of mean EW and LW of six trees in 2019.

S-shaped (Fig. S8d, e). The first and second peak of CZ and EN started on April 28 and August 18 in 2019, respectively (Fig. S8a, b). The transition from EW to LW corresponded to decreasing numbers of CZ, EN, and WT with the highest daily temperature throughout the year (Fig. S8a, b, c, f).

3.5. Temperature threshold of xylem growth

The mean temperature threshold of onset of xylem growth was 10.41°C (Fig. 8; Table S8), which was lower than the temperature where

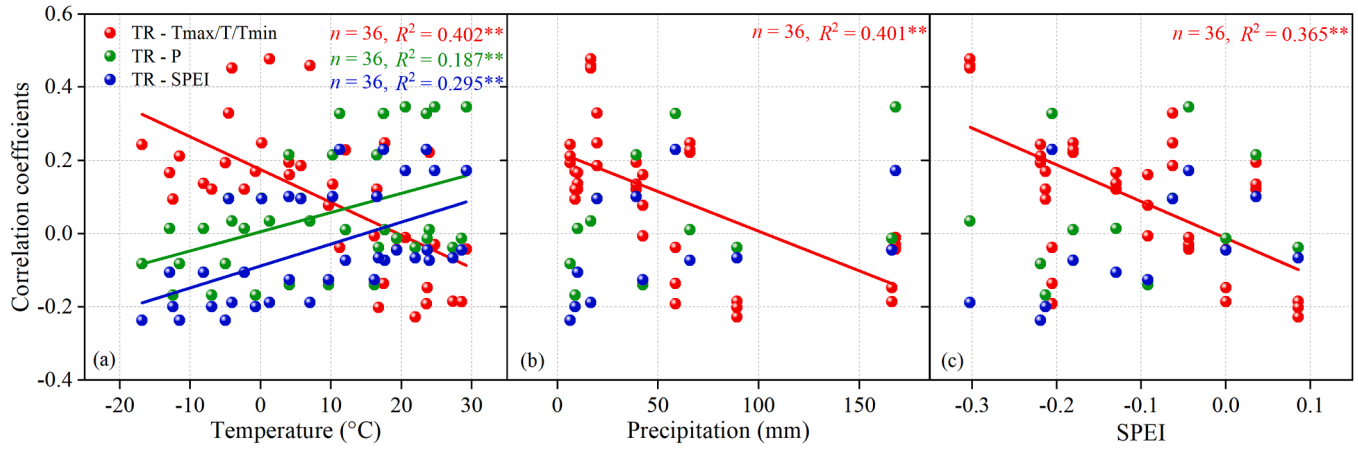

Fig. 5. The effects of the hydrothermal variables on *PS* growth-climate response at monthly scale in Shenyang. TR, total ring. Solid lines show linear regressions with statistics (n and R^2). **, $p < 0.01$.

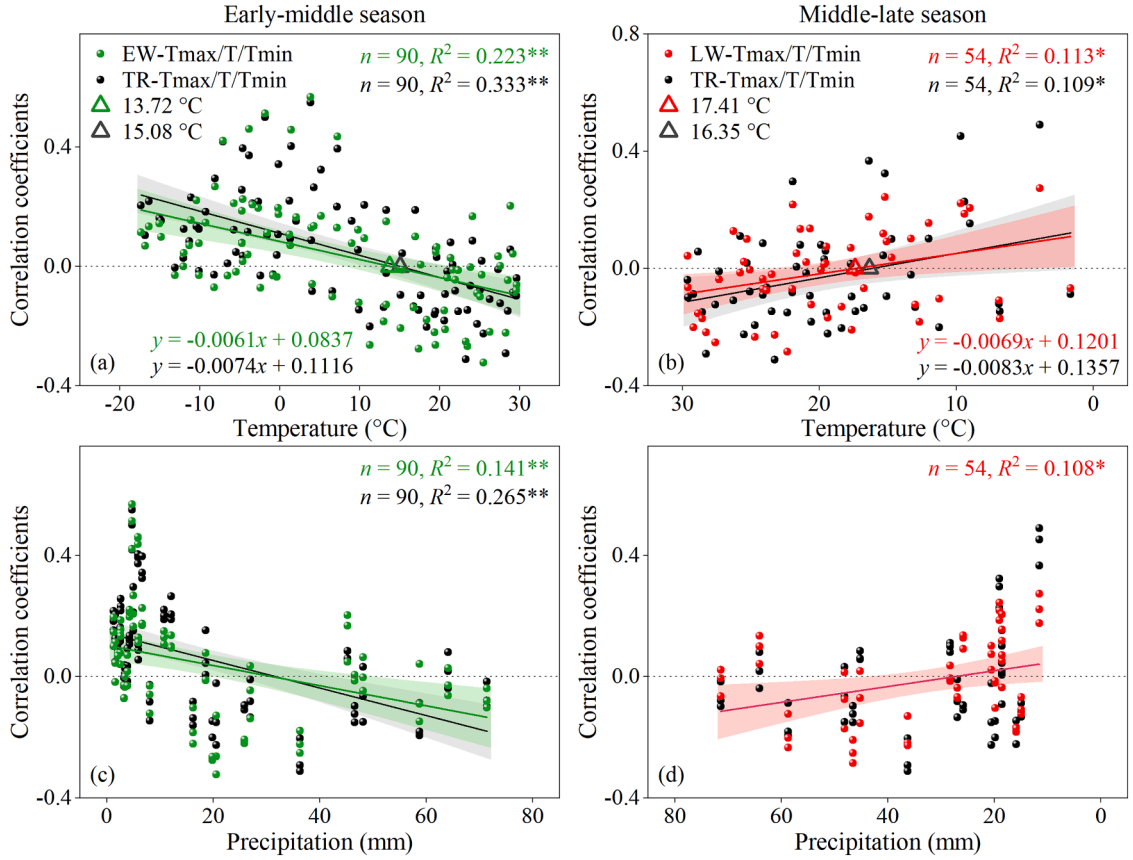

Fig. 6. The effects of the hydrothermal variables on *PS* growth-temperature response in early-middle (a, c) and middle-late (b, d) seasons at ten-day scale in Shenyang. Solid lines show linear regressions with statistics (n, R^2 and equation). The light shadings indicate the 95 % confidence intervals. Triangles represent the temperature thresholds when growth-temperature correlation shifts. The horizontal gray dashed line represents the 0 value of correlation coefficient. *, $p < 0.05$; **, $p < 0.01$.

EW-temperature response shifts in early-middle season (13.72°C). The shift date of EW growth-temperature response (May 3) is close to the occurrence date of the maximum rate of EW (May 6) (Fig. 8). The mean temperature thresholds of the end of wood production and end of xylem growth were 16.10°C and 9.84°C (Fig. 8; Table S8), respectively, which were also lower than the temperature where LW-temperature response shifts in the late season (17.41°C).

The onset of xylem growth, the end of wood production, and the end of xylem growth all occurred in early and late seasons with positive growth-temperature response while the maximum growth rate of EW and LW occurred in middle season with negative temperature-growth response (Fig. 8). These suggested that a temperature signal is needed to initiate both the onset and end of xylem growth, while water availability may affect the high growth rate of EW and LW.

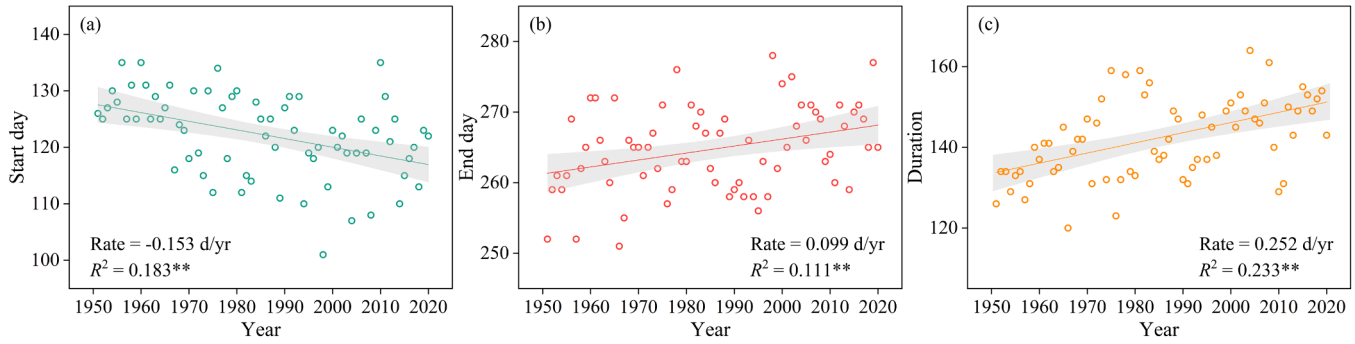

Fig. 7. The variation of the onset day (a), end day (b), and duration (c) of *PS* growth limited by water availability in a growing year from 1951 to 2020 based on response thresholds in Shenyang. The gray shading indicates the 95 % confidence interval. **, $p < 0.01$.

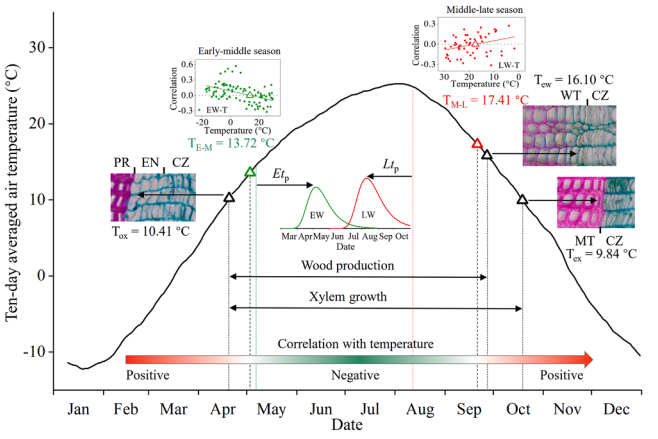

Fig. 8. The physiological processes of intra-annual shift of growth-temperature response. The black curve represents the ten-day running average of daily mean air temperatures during 1951–2020 in Shenyang. Triangles represent the temperature thresholds for the onset of xylem growth (T_{ox}), EW growth-temperature response changing from positive to negative in early-middle season (T_{E-M}), LW growth-temperature response changing from negative to positive in middle-late season (T_{M-L}), the end of wood production (T_{ew}), and the end of xylem growth (T_{ex}). Et_p (green vertical line) and Lt_p (red vertical line) represent the occurrence date of the maximum rate of EW and LW cell growth, respectively. PR, previous ring.

4. Discussion

4.1. Intra-annual rhythm of growth-climate response and the coupling effect of hydrothermal variables

PS growth-climate responses showed a dominant intra-annual rhythm in its southern range. The effects of temperature and precipitation on tree growth were coupled and synergistic in a growing year. *PS* growth was promoted by warm temperature in the early growing season (previous November–current April). The growth-temperature relationship shifted from positive to negative in May and water availability limited tree growth over summer. The similar founding about *PS* was shown in Spain, Hungary, Poland and Kazakhstan (Koprowski et al., 2012; Sánchez-Salguero et al., 2015; Kopabayeva et al., 2017; Misi et al., 2019). In late growing season (September–October), temperature promoted *PS* growth again when autumn temperature dropped. This intra-annual rhythm of growth-climate response was consistent with that based on high-density *PS* sites in the south Baltic Sea region in Europe (Harvey et al., 2020).

PS growth-climate responses in Shenyang also showed an intra-annual rhythm where temperature promoted growth in early and late growing season (i.e., winter–early spring and autumn) and inhibited growth in middle growing season (late spring–summer) (Fig. 4a). In March-April, the snow cover decreased from 50 % to nearly 0 (Fig. S1b) with mean air temperatures above 0°C in this area (Fig. S1a), which means that the snowmelt water increased and the shallow soil water content was sufficient or even excessive at this time (Baltzer et al., 2014). Thus, warm winter-spring temperature was the dominant factor for *PS* growth onset at the southern range (Balanzategui et al., 2018; Koprowski et al., 2012; Waszak et al., 2021). From late spring to summer, the rising air temperature increased evapotranspiration and led to a deficit of available water (Shestakova et al., 2017). These results were spatially coherent with *PS* growing at other areas of the southern edge (Arzac et al., 2021; Bogino et al., 2009; Bozkurt et al., 2021; Mácová, 2008; Misi et al., 2019). In cool autumn, warmer temperatures could delay the end of xylem growth (Zhang et al., 2018, 2021). Increased precipitation in autumn could decrease air temperature (Fig. S3) and, therefore, the growth responses to temperature and precipitation were opposite in late season. The intra-annual response rhythms suggested that the synergistic effects of hydrothermal variables on *PS* growth and the limiting factor can alter throughout the growing season, which provides an adequate hydrothermal management of boreal forests.

4.2. The external driver and thresholds of intra-annual rhythm of growth-climate response

Temperature was the external driver for the intra-annual rhythm of growth-climate response. The cyclic rise and fall of temperature dominated the positive and negative shift of the growth-climate relationship and temperature had stronger control on tree growth than precipitation during the cold and warm transition season. Likewise, the inter-annual shifts of tree growth-climate relationships of taiga forests in the northern hemisphere were primarily warming-driven (Matías et al., 2017; Matisons et al., 2021; Ohse et al., 2012; Wilmking et al., 2004). Temperature-induced moisture stress also contributed to reduced temperature sensitivity for *Picea glauca* at tree line in Canada (D'Arrigo et al., 2004). Moreover, temperature change along geographical gradients led to a diverging growth-climate response for conifers across Eurasia's boreal forests (Bai et al., 2019; Hellmann et al., 2016; Zhang and Wilmking, 2010). Hence, temperature not only drives inter-annual and spatial variation in the growth-climate response, but also its intra-annual rhythm. The intra-annual rhythm of growth-climate relationship could be interpreted as an adaptive response to heat cycle.

We disentangled precise intra-annual ecological thresholds using EW and LW widths with dekad climate data in Shenyang. When temperature threshold was attained in early May, the increasing temperature tended to inhibit tree growth and tree growth was mainly affected by water availability. When the temperature decreased below the threshold in late September, temperature promoted tree growth again. Furthermore, the spring growth-response threshold (13.72 °C) was higher than the mean air temperature thresholds (3–11 °C) for the onset of xylem growth of conifers in Shenyang and other cold-temperate regions

(Deslauriers et al., 2008; Jyske et al., 2014; Li et al., 2017; Rossi et al., 2007, 2008; Swidrak et al., 2011; Treml et al., 2015; Zhang et al., 2021). The autumn growth-response threshold (17.41 °C) was also higher than the thresholds for the end of cambial activity in Shenyang (16.10 °C) and other middle-high latitudes (13–15 °C) (Rossi et al., 2008; Jyske et al., 2014). These suggested that the response shift in early-middle season occurred after the onset of xylem growth and the response shift in middle-late season occurred before the end of cambium cell division.

While previous studies examined temperature threshold at inter-annual and spatial scale to explore how tree growth-climate responses shift (Bai et al., 2019; Beck et al., 2011; Bozkurt et al., 2021; D'Arrigo et al., 2004; Wilmking et al., 2004), the thresholds at intra-annual scale could infer the date and period for water availability limiting conifer growth within a year. This is particularly important under global climate change. In the intra-annual scale, the duration of *PS* growth limited by summer water availability was significantly advancing and prolonging in Shenyang (Fig. 7), suggesting that the effect of summer water availability will be more dominant when compared to the past. With climate warming, increased summer water stress will be detrimental to *PS* growth in the species' southern range. *PS* may even lose its habitat range at the southern edges, and species distribution models demonstrated a northward shift of suitable habitat in future climate scenarios (Bombi et al., 2017; Dyderski et al., 2018).

Moreover, these thresholds play a key role in guiding forest management to increase wood production and carbon storage at the southern edges of boreal conifer distribution. For instance, water should be replenished in spring when the daily mean temperature rises to 13.72°C to delay reaching the threshold and improve earlywood cell production. When the daily mean temperature in autumn drops to 17.41°C, cold protection measures should be taken to delay the end of cambial activity and increase wood cell production.

4.3. The physiological mechanisms of intra-annual rhythm of growth-climate response

The pattern of cambial activity reflected the response of trees to local intra-annual climate change (Martínez del Castillo et al., 2016; Fajstavr et al., 2020). The bimodal pattern of cambial activity in Shenyang in 2019, with two peaks in spring (April-May) and summer (August) was distinct from the unimodal pattern of *PS* at Spain, France, and Austria sites in previous studies (Camarero et al., 2010; Cuny et al., 2012; Oberhuber et al., 2014). The intra-annual distribution of precipitation in 2019 (Fig. S8f), with August (447 mm) receiving more than twice as much precipitation as July (108 mm). The second peak of cambial activity seemed to be closely associated with high precipitation in August following low precipitation in July in 2019. Summer drought caused reduction or cessation of cambial activity, followed by the restoration of active cambial production induced by precipitation occurring in late-summer or autumn (Balzano et al., 2018; De Micco et al, 2016). This reflected the ability of tree to respond to favorable environmental conditions at the end of the growing season (Oberhuber et al., 2021).

The intra-annual dynamic of growth-climate relationship corresponded to cambial activity and xylogenesis well. From winter to early spring, triggering cambial resumption and xylem growth requires a temperature signal after dormancy (Deslauriers et al., 2008; Huang et al., 2020; Rossi et al., 2007). Although the cambium of *PS* remained dormant in winter (November-February) (Fig. 4c), warmer temperatures might reduce the risk of freezing damage (Kopabayeva et al., 2017) and boost photosynthetic capacity of evergreen conifers (Matisons et al., 2021; Michelot et al., 2012), which accumulate carbohydrates for subsequent growth (Nippert et al., 2004). Warm temperature in early spring (March-April) could promote snow melting and replenish soil water (Fig. S1b), providing suitable hydrothermal conditions for cambial resumption and xylem growth. Therefore, temperature in early season contributed to a strong beneficial effect on tree growth.

The positive-negative shift of growth-temperature response in early-middle season was linked to the strong water demand for the rapid EW cell formation. In early May, cambium cells divided rapidly and EW growth reached its maximum rate (Fig. S8a, f), when a sufficient water supply is required to maintain the turgor pressure for cambium cell division and expansion (Steppe et al., 2015; Vieira et al., 2014). However, the winter snowmelt water has infiltrated and evaporated in late spring, and the summer monsoon precipitation has not yet arrived. Increasing temperatures at this time can exacerbate soil moisture loss with increasing evapotranspiration (Kopabayeva et al., 2017), which constrained cell production (Rahman et al., 2019). The close proximity between EW-temperature response shift (May 3) and maximum EW growth rate (May 6) further supported our speculation. Thus, EW had a negative response to temperature and a positive response to precipitation in May.

The negative-positive shift of growth-temperature response in middle-late season was associated with the heat requirement for cambial cell division. The growth rate of EW and LW in turn reached its maximum rate in May and August (Fig. 4e), which required a large amount of available water, so the high temperature in middle season was not conducive to tree growth. In this time, the transition from EW to LW was also related to water availability (Arzac et al., 2021; Netsvetov et al., 2021). With temperature decrease in September-October, the cambium began to enter dormant state and wood production had weakened (Fig. S8), temperature again became a critical factor limiting tree growth in late season. Warmer weather could prolong the cambium activity and xylem growth in wet and cold regions (Li et al., 2017; Rossi et al., 2008). The shift of LW-temperature response from negative to positive was synchronous with the end of cambial cell division (September 21), which also suggests both processes were associated.

4.4. Limitations

Based on the 18 sites in previous dendrochronological and our studies, we found the dominant intra-annual pattern of *PS* growth-climate response at its southern distribution limits. Although *PS* climate-growth response is similar between our site and the rest of 17 sites, we expect there are greater variation in climate-growth relationship due to geographic varieties and local habitat conditions (Carlisle and Brown, 1968; Cedro et al., 2022; Klisz et al., 2023) when considering the entire distribution range. At other *PS* southern sites, temperature thresholds of intra-annual response shift also exist, but the values of thresholds may slightly differ from that in Shenyang due to local climate conditions. The phenological monitoring in this study was carried out in 2019, with mean temperature and precipitation at average levels for the past 60 years, which can represent the general pattern of cambial phenology and xylem growth in Shenyang. The phenological dates of *PS* at Shenyang site was also basically consistent with that at other sites in the southern distribution region (Gruber et al., 2010; Cuny et al., 2012; Swidrak et al., 2014; Martínez del Castillo et al., 2016). However, cambial activity of trees is affected by many factors, such as site topography and soil conditions (Oberhuber et al., 2014; Martínez del Castillo et al., 2016; Zhang et al., 2018). And it can vary among years (Swidrak et al., 2014; Zhang et al., 2021). Therefore, we advise future studies should take these factors into account as variation in phenology, which could also play an important role in the length of wood production and carbon sequestration.

5. Summary and outlook

Although many dendrochronological studies on *PS* in a variety of ecological conditions have been conducted, the main intra-annual rhythms of response received less attention and remained a key knowledge gap. Our study found a broad-scale dominant intra-annual rhythm of *PS* growth-climate response at its southern distribution limits, despite the variability existing among sites. The coupling effects of temperature and precipitation was detected on *PS* growth within a

growing year. Due to a similar intra-annual relationship pattern at local (Shenyang site) and regional scales, we conducted mechanistic examination on *PS* physiological responses in Shenyang. Temperature was the external driver for controlling the intra-annual rhythm of growth-climate responses, and the thresholds for response shifts in spring and autumn were identified in Shenyang. The response shift in spring-summer was related to a sharp water demand at the rapid growth of earlywood cells, and that in summer-autumn was related to the heat demand for cambial cell division. Despite mechanistic exploration was only conducted at Shenyang site within one growing season, the intra-annual rhythm of *PS* growth-climate response provided a new perspective and reference for boreal forest growth. We hope that this study instigates further exploration on the intra-annual pattern of tree growth-climate responses at larger scale. Additionally, we recommend a multi-site and multi-year investigation of cambial phenology and xylem dynamic that could better disentangle intra-annual growth rhythm.

Funding

This work was supported by the (41888101, 41871027, 41601045, 41571094, 31570632) and the Post-doctoral Research Start-up Fund of Shenyang Agricultural University (X2021044).

CRediT authorship contribution statement

Junxia Li: Conceptualization, Data curation, Investigation, Visualization, Writing – original draft, Formal analysis. **Yuting Jin:** Data curation, Investigation. **Ying Zhao:** Investigation. **Tsun Fung Au:** Conceptualization, Writing – review & editing. **Yucheng Wang:** Funding acquisition, Writing – review & editing. **Zhenju Chen:** Conceptualization, Funding acquisition, Writing – review & editing.

Declaration of Competing Interest

The authors declare that they have no known competing financial interests or personal relationships that could have appeared to influence the work reported in this paper.

Data availability

Data will be made available on request.

Acknowledgements

We thank Feng Li, Jingyuan Zhang, Jiayang Chen, Sen Hou, Zi'ang Xin for field work. We thank Zhiyan Wang, Linlin Chen, Yifei Zhang, Erxin Shang, Yinyi Chen, Ye Zhang for data collection. We thank Xin Gao for proof reading on an earlier version of the manuscript.

Supplementary materials

Supplementary material associated with this article can be found, in the online version, at doi:10.1016/j.agrformet.2023.109871.

References

Agafonov, L.I., Gurskaya, M.A., Kukarskih, V.V., Bubnov, M.O., Devi, N.M., Galimova, A. A., 2021. Insular pine forests of the Southern Urals and ribbon pine forests of the Altai as objects of dendroclimatic research. Russ. J. Ecol. 52, 349–357. https://doi.org/10.1134/s1067413621050039.

Allen, C.D., Macalady, A.K., Chenchouni, H., Bachelet, D., McDowell, N.G., Vennetier, M., Kitzberger, T., Rigling, A., Breshears, D.D., Hogg, E.H., Gonzalez, P., Fensham, R.J., Zhang, Z., Castro, J., Demidova, N.A., Lim, J., Allard, G., Running, S. W., Semerci, A., Cobb, N.S., 2010. A global overview of drought and heat-induced tree mortality reveals emerging climate change risks for forests. Forest Ecol. Manag. 259, 660–684. https://doi.org/10.1016/j.foreco.2009.09.001.

Arzac, A., Tabakova, M.A., Khotcinskaia, K., Koteneva, A., Kirdyanov, A.V., Olano, J.M., 2021. Linking tree growth and intra-annual density fluctuations to climate in suppressed and dominant *Pinus sylvestris* L. trees in the forest-steppe of Southern Siberia. Dendrochronologia 67, 125842. https://doi.org/10.1016/j.dendro.2021.125842.

Babst, F., Bouriaud, O., Poulter, B., Trouet, V., Girardin, M.P., Frank, D.C., 2019. Twentieth century redistribution in climatic drivers of global tree growth. Sci. Adv. 5, eaat4313. https://doi.org/10.1126/sciadv.aat4313.

Bai, X., Zhang, X., Li, J., Duan, X., Jin, Y., Chen, Z., 2019. Altitudinal disparity in growth of Dahurian larch (Larix gmelinii Rupr.) in response to recent climate change in northeast China. Sci. Total Environ. 670, 466–477. https://doi.org/10.1016/j.scitotenv.2019.03.232.

Balanzategui, D., Knorr, A., Heussner, K.U., Ważny, T., Beck, W., Słowiński, M., Helle, G., Buras, A., Wilmking, M., van der Maaten, E., Scharnweber, T., Dorado-Liñán, I., Heinrich, I., 2018. An 810-year history of cold season temperature variability for northern Poland. Boreas 47, 443–453. https://doi.org/10.1111/bor.1227.

Baltzer, J.L., Veness, T., Chasmer, L.E., Sniderhan, A.E., Quinton, W.L., 2014. Forests on thawing permafrost: fragmentation, edge effects, and net forest loss. Glob. Chang. Biol. 20, 824–834. https://doi.org/10.1111/gcb.12349.

Balzano, A., Čufar, K., Battipaglia, G., Merela, M., Prislan, P., Aronne, G., De Micco, V., 2018. Xylogenesis reveals the genesis and ecological signal of IADFs in Pinus pinea L. and Arbutus unedo L. Ann. Bot. 121, 1231–1242. https://doi.org/10.1093/aob/mcy008.

Beck, P.S.A., Juday, G.P., Alix, C., Barber, V.A., Winslow, S.E., Sousa, E.E., Heiser, P., Herriges, J.D., Goetz, S.J., 2011. Changes in forest productivity across Alaska consistent with biome shift. Ecol. Lett. 14, 373–379. https://doi.org/10.1111/j.1461-0248.2011.01598.x.

Bogino, S., Fernández Nieto, M.J., Bravo, F., 2009. Climate effect on radial growth of *Pinus sylvestris* at its southern and western distribution limits. Silva Fenn. 43, 609–623. https://doi.org/10.14214/sf.183.

Bombi, P., D'Andrea, E., Rezaie, N., Cammarano, M., Matteucci, G., 2017. Which climate change path are we following? Bad news from Scots pine. PLoS One 12, e0189468. https://doi.org/10.1371/journal.pone.0189468.

Bozkurt, A.E., Sahan, E.A., Köse, N., 2021. Growth responses of *Pinus sylvestris* L. to climate from the southeastern limit of its natural distribution area, Turkey. Dendrochronologia 70, 125897. https://doi.org/10.1016/j.dendro.2021.125897.

Camarero, J.J., Olano, J.M., Parras, A., 2010. Plastic bimodal xylogenesis in conifers from continental Mediterranean climates. New Phytol. 185, 471–480. https://doi.org/10.1111/j.1469-8137.2009.03073.x.

Carlisle, A., Brown, A.H.F., 1968. Biological flora of the British Isles: *Pinus sylvestris* L. J. Ecol. 56, 269–307. https://doi.org/10.2307/2258078.

Cedro, A., Cedro, B., Podlasiński, M., 2022. Differences in growth–climate relationships among scots pines growing on various dune generations on the southern baltic coast. Forests 13, 470. https://doi.org/10.3390/f13030470.

Ciais, P., Reichstein, M., Viovy, N., Granier, A., Ogée, J., Allard, V., Aubinet, M., Buchmann, N., Bernhofer, C., Carrara, A., Chevallier, F., Noblet, N.D., Friend, A.D., Friedlingstein, P., Grünwald, T., Heinesch, B., Keronen, P., Knohl, A., Krinner, G., Loustau, D., Manca, G., Matteucci, G., Miglietta, F., Ourcival, J., Papale, D., Pilegaard, K., Rambal, S., Seufert, G., Soussana, J., Sanz, M.J., Schulze, E., Vesala, T., Valentini, R., 2005. Europe-wide reduction in primary productivity caused by the heat and drought in 2003. Nature 437, 529–533. https://doi.org/10.1038/nature03972.

Cook, E.R., Kairiukstis, L.A., 1990. Methods of dendrochronology: Applications in the Environmental Sciences. Kluwer Academic Publishers, p. 394.

Cuny, H.E., Rathgeber, C.B., Frank, D.C., Fonti, P., Mäkinen, H., Prislan, P., Rossi, S., del Castillo, E.M., Campelo, F., Vavrčík, H., Camarero, J.J., Bryukhanova, M.V., Jyske, T., Gričar, J., Gryc, V., de Luis, M., Vieira, J., Čufar, K., Kirdyanov, A.V., Oberhuber, W., Treml, V., Huang, J., Li, X., Swidrak, I., Deslauriers, A., Liang, E., Nöjd, P., Gruber, A., Nabais, C., Morin, H., Krause, C., King, G., Fournier, M., 2015. Woody biomass production lags stem-girth increase by over one month in coniferous forests. Nat. Plants 1, 15160. https://doi.org/10.1038/nplants.2015.160.

Cuny, H.E., Rathgeber, C.B., Lebourgeois, F., Fortin, M., Fournier, M., 2012. Life strategies in intra-annual dynamics of wood formation: example of three conifer species in a temperate forest in north-east France. Tree Physiol. 32, 612–625. https://doi.org/10.1093/treephys/tps039.

D'Arrigo, R.D., Kaufmann, R.K., Davi, N., Jacoby, G.C., Laskowski, C., Myneni, R.B., Cherubini, P., 2004. Thresholds for warming-induced growth decline at elevational tree line in the Yukon Territory. Canada. Glob. Biogeochem. Cycles 18, gb3021. https://doi.org/10.1029/2004 gb002249.

De Micco, V., Balzano, A., Čufar, K., Aronne, G., Gričar, J., Merela, M., Battipaglia, G., 2016. Timing of false ring formation in Pinus halepensis and Arbutus unedo in Southern Italy: outlook from an analysis of xylogenesis and tree-ring chronologies. Front. Plant Sci. 7, 705. https://doi.org/10.3389/fpls.2016.00705.

Denne, M.P., 1988. Definition of latewood according to Mork (1928). IAWA J. 10, 59–61. https://doi.org/10.1163/22941932-90001112.

Deslauriers, A., Morin, H., Begin, Y., 2003. Cellular phenology of annual ring formation of Abies balsamea in the Quebec boreal forest (Canada). Can. J. For. Res. 33, 190–200. https://doi.org/10.1139/x02-178.

Deslauriers, A., Rossi, S., Anfodillo, T., Saracino, A., 2008. Cambial phenology, wood formation and temperature thresholds in two contrasting years at high altitude in southern Italy. Tree Physiol. 28, 863–871. https://doi.org/10.1093/treephys/28.6.863.

D'Orangeville, L., Duchesne, L., Houle, D., Kneeshaw, D.D., Côté, B., Pederson, N., 2016. Northeastern North America as a potential refugium for boreal forests in a warming climate. Science 352, 1452–1455. https://doi.org/10.1126/science.aaf4951.

Durrant, T.H., De Rigo, D., Caudullo, G., 2016. *Pinus sylvestris* in Europe: distribution, habitat, usage and threats. European Atlas of Forest Tree Species. Publication Office of the European Union, Luxembourg, pp. 132–133.

Dyderski, M.K., Paź, S., Frelich, L.E., Jagodziński, A.M., 2018. How much does climate change threaten European forest tree species distributions? Glob. Change Biol. 24, 1150–1163. https://doi.org/10.1111/gcb.13925.

Fajstavr, M., Giagli, K., Vavrčík, H., Gryc, V., Horáček, P., Urban, J., 2020. The cambial response of Scots pine trees to girdling and water stress. IAWA J. 41, 159–185. https://doi.org/10.1163/22941932-bja10004.

Gilliam, F.S., 2016. Forest ecosystems of temperate climatic regions: from ancient use to climate change. New Phytol. 212, 871–887. https://doi.org/10.1111/nph.14255.

Gričar, J., Zupančič, M., Čufar, K., Koch, G., Schmitt, U., Oven, P., 2006. Effect of local heating and cooling on cambial activity and cell differentiation in the stem of Norway spruce (Picea abies). Ann. Bot. 97, 943–951. https://doi.org/10.1093/aob/mcl050.

Gruber, A., Strobl, S., Veit, B., Oberhuber, W., 2010. Impact of drought on the temporal dynamics of wood formation in *Pinus sylvestris*. Tree Physiol. 30, 490–501. https://doi.org/10.1093/treephys/tpq003.

Harvey, J.E., Smiljanić, M., Scharnweber, T., Buras, A., Cedro, A., Cruz-García, R., Drobyshev, I., Janecka, K., Jansons, Ā., Kaczka, R.J., Klisz, M., Läänelaid, A., Matisons, R., Muffler, L., Sohar, K., Spyt, B., Stolz, J., van der Maaten, E., van der Maaten-Theunissen, M., Vitas, A., Weigel, R., Kreyling, J., Wilmking, M., 2020. Tree growth influenced by warming winter climate and summer moisture availability in northern temperate forests. Glob. Change Biol. 26, 2505–2518. https://doi.org/10.1111/gcb.14966.

Hellmann, L., Agafonov, L., Ljungqvist, F.C., Churakova, O., Düthorn, E., Esper, J., Hülsman, L., Kirdyanov, A.V., Moiseev, P., Myglan, V.S., Nikolaev, A.N., Reinig, F., Schweingruber, F.H., Solomina, O., Tegel, W., Büntgen, U., 2016. Diverse growth trends and climate responses across Eurasia's boreal forest. Environ. Res. Lett. 11, 074021 https://doi.org/10.1088/1748-9326/11/7/074021.

Holmes, R.L., 1983. Computer-assisted quality control in tree-ring dating and measurement. Tree-Ring Bull. 43, 69–78.

Huang, J., Deslauriers, A., Rossi, S., 2014. Xylem formation can be modeled statistically as a function of primary growth and cambium activity. New Phytol. 203, 831–841. https://doi.org/10.1111/nph.12859.

Huang, J., Guo, X., Rossi, S., Zhai, L., Yu, B., Zhang, S., Zhang, M., 2018. Intra-annual wood formation of subtropical Chinese red pine shows better growth in dry season than wet season. Tree Physiol. 38, 1225–1236. https://doi.org/10.1093/treephys/tpy046.

Huang, J., Ma, Q., Rossi, S., Biondi, F., Deslauriers, A., Fonti, P., Liang, E., Mäkinen, H., Oberhuber, W., Rathgeber, C.B., Tognetti, R., Treml, V., Yang, B., Zhang, J., Antonucci, S., Bergeron, Y., Camarero, J.J., Campelo, F., Čufar, K., Cuny, H.E., de Luis, M., Giovannelli, A., Gričar, J., Gruber, A., Gryc, V., Güney, A., Guo, X., Huang, W., Jyske, T., Kašpar, J., King, G., Krause, C., Lemay, A., Liu, F., Lombardi, F., Martínez del Castillo, E., Morin, H., Nabais, C., Nöjd, P., Peters, R.L., Prislan, P., Saracino, A., Swidrak, I., Vavrčík, H., Vieira, J., Yu, B., Zhang, S., Zeng, Q., Zhang, Y., Ziaco, E., 2020. Photoperiod and temperature as dominant environmental drivers triggering secondary growth resumption in Northern Hemisphere conifers. Proc. Natl. Acad. Sci. 117, 20645–20652. https://doi.org/10.1073/pnas.2007058117.

Huang, N., Song, Y., Wang, J., Zhang, Z., Ma, S., Jiang, K., Pan, Z., 2022. Climatic threshold of crop production and climate change adaptation: a case of winter wheat production in China. Front. Ecol. Evol. 10, 1019436 https://doi.org/10.3389/fevo.2022.1019436.

Jyske, T., Mäkinen, H., Kalliokoski, T., Nöjd, P., 2014. Intraannual tracheid production of Norway spruce and Scots pine across a latitudinal gradient in Finland. Agric. For. Meteorol. 194, 241–254. https://doi.org/10.1016/j.agrformet.2014.04.015.

Klisz, M., Puchałka, R., Jakubowski, M., Koprowski, M., Netsvetov, M., Prokopuk, Y., Jevšenak, J., 2023. Local site conditions reduce interspecific differences in climate sensitivity between native and non-native pines. Agric. For. Meteorol. 341, 109694 https://doi.org/10.1016/j.agrformet.2023.109694.

Kolář, T., Kusbach, A., Čermák, P., Štěrba, T., Batkhuu, E., Rybníček, M., 2020. Climate and wildfire effects on radial growth of *Pinus sylvestris* in the Khan Khentii Mountains, north-central Mongolia. J. Arid Environ. 182, 104223 https://doi.org/10.1016/j.jaridenv.2020.104223.

Kopabayeva, A., Mazarzhanova, K., Köse, N., Akkemik, Ü., 2017. Tree-ring chronologies of *Pinus sylvestris* from Burabai Region (Kazakhstan) and their response to climate change. Dendrobiology 78, 96–110. https://doi.org/10.12657/denbio.078.010.

Koprowski, M., Przybylak, R., Zielski, A., Pospieszyńska, A., 2012. Tree rings of Scots pine (*Pinus sylvestris* L.) as a source of information about past climate in northern Poland. Int. J. Biometeorol. 56, 1–10. https://doi.org/10.1007/s00484-010-0390-5.

Kuznetsova, V.V., Solomina, O.N., 2022. Contrasting climate signals across a Scots pine (*Pinus sylvestris* L.) tree-ring network in the Middle Volga (European Russia). Dendrochronologia 73, 125957. https://doi.org/10.1016/j.dendro.2022.125957.

Li, J., Bai, X., Zhang, X., Chang, Y., Lu, X., Zhao, X., Chen, Z., 2017a. Different responses of natural *Pinus sylvestris* var. mongolica growth to climate change in southern and northern forested areas in the Great Xing'an Mountains. Acta Ecol. Sin. 37, 7232–7241. https://doi.org/10.5846/stxb201608131660.

Li, X., Liang, E., Gričar, J., Rossi, S., Cufar, K., Ellison, A.M., 2017b. Critical minimum temperature limits xylogenesis and maintains treelines on the southeastern Tibetan Plateau. Sci. Bull. 62, 804–812. https://doi.org/10.1016/j.scib.2017.04.025.

Lindner, M., Fitzgerald, J., Zimmermann, N.E., Reyer, C.P., Delzon, S., van der Maaten, E., Schelhaas, M., Lasch, P., Eggers, J., van der Maaten-Theunissen, M., Suckow, F., Psomas, A., Poulter, B.I., Hanewinkel, M., 2014. Climate change and European forests: what do we know, what are the uncertainties, and what are the implications for forest management? J. Environ. Manag. 146, 69–83. https://doi.org/10.1016/j.jenvman.2014.07.030.

Lupi, C., Morin, H., Deslauriers, A., Rossi, S., 2010. Xylem phenology and wood production: resolving the chicken-or-egg dilemma. Plant Cell Environ. 33, 1721–1730. https://doi.org/10.1111/j.1365-3040.2010.02176.x.

Mácová, M., 2008. Dendroclimatological comparison of native *Pinus sylvestris* and invasive Pinus strobus in different habitats in the Czech Republic. Preslia 80, 277–289.

Martin-Benito, D., Beeckman, H., Cañellas, I., 2013. Influence of drought on tree rings and tracheid features of Pinus nigra and *Pinus sylvestris* in a mesic Mediterranean forest. Eur. J. For. Res. 132, 33–45. https://doi.org/10.1007/s10342-012-0652-3.

Martínez del Castillo, E., Longares, L.A., Gričar, J., Prislan, P., Gil-Pelegrín, E., Čufar, K., de Luis, M., 2016. Living on the edge: contrasted wood-formation dynamics in Fagus sylvatica and *Pinus sylvestris* under mediterranean conditions. Front. Plant Sci. 7, 370. https://doi.org/10.3389/fpls.2016.00370.

Matías, L., Linares, J.C., Sanchez-Miranda, A., Jump, A.S., 2017. Contrasting growth forecasts across the geographical range of Scots pine due to altitudinal and latitudinal differences in climatic sensitivity. Glob. Change Biol. 23, 4106–4116. https://doi.org/10.1111/gcb.13627.

Matisons, R., Elferts, D., Krišāns, O., Schneck, V., Gärtner, H., Bast, A., Wojda, T., Kowalczyk, J., Jansons, Ā., 2021. Non-linear regional weather-growth relationships indicate limited adaptability of the eastern Baltic Scots pine. Forest Ecol. Manag. 479, 118600 https://doi.org/10.1016/j.foreco.2020.118600.

Michelot, A., Breda, N., Damesin, C., Dufrene, E., 2012. Differing growth responses to climatic variations and soil water deficits of Fagus sylvatica, Quercus petraea and *Pinus sylvestris* in a temperate forest. Forest Ecol. Manag. 265, 161–171. https://doi.org/10.1016/j.foreco.2011.10.024.

Misi, D., Náfrádi, K., 2017. Growth response of Scots pine to changing climatic conditions over the last 100 years: a case study from Western Hungary. Trees-Struct. Funct. 31, 919–928. https://doi.org/10.1007/s00468-016-1517-z.

Misi, D., Puchałka, R., Pearson, C., Robertson, I., Koprowski, M., 2019. Differences in the climate-growth relationship of Scots pine: a case study from Poland and Hungary. Forests 10, 243. https://doi.org/10.3390/f10030243.

Nagavciuc, V., Roibu, C., Ionita, M., Mursa, A., Cotos, M., Popa, I., 2019. Different climate response of three tree ring proxies of *Pinus sylvestris* from the Eastern Carpathians, Romania. Dendrochronologia 54, 56–63. https://doi.org/10.1016/j.dendro.2019.02.007.

Netsvetov, M., Prokopuk, Y., Ivanko, I., Kotovych, O., Romenskyy, M., 2021. Quercus robur survival at the rear edge in steppe: dendrochronological evidence. Dendrochronologia 67, 125843. https://doi.org/10.1016/j.dendro.2021.125843.

Nippert, J.B., Duursma, R.A., Marshall, J.D., 2004. Seasonal variation in photosynthetic capacity of montane conifers. Funct. Ecol. 18, 876–886. https://doi.org/10.1111/j.0269-8463.2004.00909.x.

Oberhuber, W., Gruber, A., Kofler, W., Swidrak, I., 2014. Radial stem growth in response to microclimate and soil moisture in a drought-prone mixed coniferous forest at an inner Alpine site. Eur. J. For. Res. 133, 467–479. https://doi.org/10.1007/s10342-013-0777-z.

Oberhuber, W., Landlinger-Weilbold, A., Schröter, D.M., 2021. Triggering bimodal radial stem growth in *Pinus sylvestris* at a drought-prone site by manipulating stem carbon availability. Front. Plant Sci. 12, 674438 https://doi.org/10.3389/fpls.2021.674438.

Ohse, B., Jansen, F., Wilmking, M., 2012. Do limiting factors at Alaskan treelines shift with climatic regimes? Environ. Res. Lett. 7, 015505 https://doi.org/10.1088/1748-9326/7/1/015505.

Pan, Y., Birdsey, R., Fang, J., Houghton, R.A., Kauppi, P.E., Kurz, W.A., Phillips, O.L., Shvidenko, A., Lewis, S.L., Canadell, J.G., Ciais, P., Jackson, R.B., Pacala, S.W., McGuire, A.D., Piao, S., Rautiainen, A., Sitch, S.A., Hayes, D.J., 2011. A large and persistent carbon sink in the World's forests. Science 333, 988–993. https://doi.org/10.1126/science.1201609.

Qi, C., Jiao, L., Xue, R., Wu, X., Du, D., 2022. Timescale effects of radial growth responses of two dominant coniferous trees on climate change in the eastern Qilian Mountains. Forests 13, 72. https://doi.org/10.3390/f13010072.

Rahman, M.H., Nugroho, W.D., Nakaba, S., Kitin, P., Kudo, K., Yamagishi, Y., Begum, S., Marsoem, S.N., Funada, R., 2019. Changes in cambial activity are related to precipitation patterns in four tropical hardwood species grown in Indonesia. Am. J. Bot. 106, 760–771. https://doi.org/10.1002/ajb2.1297.

Rathgeber, C.B., Rossi, S., Bontemps, J.D., 2011. Cambial activity related to tree size in a mature silver-fir plantation. Ann. Bot. 108, 429–438. https://doi.org/10.1093/aob/mcr168.

Richardson, A.D., Keenan, T.F., Migliavacca, M., Ryu, Y., Sonnentag, O., Toomey, M., 2013. Climate change, phenology, and phenological control of vegetation feedbacks to the climate system. Agric. For. Meteorol. 169, 156–173. https://doi.org/10.1016/j.agrformet.2012.09.012.

Rossi, S., Anfodillo, T., Menardi, R., 2006a. Trephor: a new tool for sampling microcores from tree stems. IAWA J. 27, 89–97. https://doi.org/10.1163/22941932-90000139.

Rossi, S., Anfodillo, T., Čufar, K., Cuny, H.E., Deslauriers, A., Fonti, P., Frank, D.C., Gričar, J., Gruber, A., Huang, J., 2016. Pattern of xylem phenology in conifers of cold ecosystems at the Northern Hemisphere. Glob. Change Biol. 22, 3804–3813. https://doi.org/10.1111/gcb.13317.

Rossi, S., Deslauriers, A., Anfodillo, T., 2006b. Assessment of cambial activity and xylogenesis by microsampling tree species: an example at the alpine timberline. IAWA J. 27, 383–394. https://doi.org/10.1163/22941932-90000161.

Rossi, S., Deslauriers, A., Anfodillo, T., Carraro, V., 2007. Evidence of threshold temperatures for xylogenesis in conifers at high altitudes. Oecologia 152, 1–12. https://doi.org/10.1007/s00442-006-0625-7.

Rossi, S., Deslauriers, A., Gričar, J., Seo, J., Rathgeber, C.B., Anfodillo, T., Morin, H., Levanič, T., Oven, P., Jalkanen, R., 2008. Critical temperatures for xylogenesis in conifers of cold climates. Glob. Ecol. Biogeogr. 17, 696–707. https://doi.org/10.1111/j.1466-8238.2008.00417.x.

Rossi, S., Deslauriers, A., Morin, H., 2003. Application of the Gompertz equation for the study of xylem cell development. Dendrochronologia 21, 33–39. https://doi.org/10.1078/1125-7865-00034.

Rossi, S., Girard, M.J., Morin, H., 2014. Lengthening of the duration of xylogenesis engenders disproportionate increases in xylem production. Glob. Change Biol. 20, 2261–2271. https://doi.org/10.1111/gcb.12470.

Safford, H.D., Vallejo, V.R., 2019. Chapter 12: ecosystem management and ecological restoration in the anthropocene: integrating global change, soils, and disturbance in boreal and mediterranean forests. Developments in Soil Science. Elsevier, pp. 259–308. https://doi.org/10.1016/b978-0-444-63998-1.00012-4, 36.

Sánchez-Salguero, R., Camarero, J.J., Hevia, A., Madrigal-González, J., Linares, J.C., 2015. What drives growth of Scots pine in continental Mediterranean climates: drought, low temperatures or both? Agric. For. Meteorol. 206, 151–162. https://doi.org/10.1016/j.agrformet.2015.03.004.

Schaphoff, S., Reyer, C.P., Schepaschenko, D., Gerten, D., Shvidenko, A., 2016. Tamm review: observed and projected climate change impacts on Russia's forests and its carbon balance. Forest Ecol. Manag. 361, 432–444. https://doi.org/10.1016/j.foreco.2015.11.043.

Shestakova, T.A., Voltas, J., Saurer, M., Siegwolf, R.T., Kirdyanov, A.V., 2017. Warming effects on *Pinus sylvestris* in the cold-dry Siberian forest-steppe: positive or negative balance of trade? Forests 8, 490. https://doi.org/10.3390/f8120490.

Stahle, D.W., Cleaveland, M.K., Grissino-Mayer, H.D., Griffin, R.D., Fye, F.K., Therrell, M. D., Burnette, D.J., Meko, D.M., Díaz, J.V., 2009. Cool and warm season precipitation reconstructions over Western New Mexico. J. Clim. 22, 3729–3750. https://doi.org/10.1175/2008jcli2752.1.

Steppe, K., Sterck, F., Deslauriers, A., 2015. Diel growth dynamics in tree stems: linking anatomy and ecophysiology. Trends Plant Sci. 20, 335–343. https://doi.org/10.1016/j.tplants.2015.03.015.

Stokes, M.A., Smiley, T.L., 1968. An Introduction to Tree Ring Dating. University of Chicago Press, p. 73.

Swidrak, I., Gruber, A., Kofler, W., Oberhuber, W., 2011. Effects of environmental conditions on onset of xylem growth in *Pinus sylvestris* under drought. Tree Physiol. 31, 483–493. https://doi.org/10.1093/treephys/tpr034.

Swidrak, I., Gruber, A., Oberhuber, W., 2014. Xylem and phloem phenology in co-occurring conifers exposed to drought. Trees-Struct. Funct. 28, 1161–1171. https://doi.org/10.1007/s00468-014-1026-x.

Tabakova, M.A., Arzac, A., Martínez, E., Kirdyanov, A.V., 2020. Climatic factors controlling *Pinus sylvestris* radial growth along a transect of increasing continentality in Southern Siberia. Dendrochronologia 62, 125709. https://doi.org/10.1016/j.dendro.2020.125709.

Treml, V., Kašpar, J., Kuželová, H., Gryc, V., 2015. Differences in intra-annual wood formation in Picea abies across the treeline ecotone, Giant Mountains, Czech Republic. Trees-Struct. Funct. 29, 515–526. https://doi.org/10.1007/s00468-014-1129-4.

Vieira, J., Rossi, S., Campelo, F., Freitas, H., Nabais, C., 2014. Xylogenesis of Pinus pinaster under a Mediterranean climate. Ann. For. Sci. 71, 71–80. https://doi.org/10.1007/s13595-013-0341-5.

Waszak, N., Robertson, I., Puchałka, R., Przybylak, R., Pospieszyńska, A., Koprowski, M., 2021. Investigating the climate-growth response of Scots pine (*Pinus sylvestris* L.) in Northern Poland. Atmosphere 12, 1690. https://doi.org/10.3390/atmos12121690.

Wigley, T.M.L., Briffa, K.R., Jones, P.D., 1984. On the average value of correlated time series, with applications in dendroclimatology and hydrometeorology. J. Appl. Meteorol. Climatol. 23, 201–213. https://doi.org/10.1175/1520-0450(1984)023<0201:otavoc>2.0.co;2.

Wilmking, M., Juday, G.P., Barber, V.A., Zald, H.S.J., 2004. Recent climate warming forces contrasting growth responses of white spruce at tree line in Alaska through temperature thresholds. Glob. Change Biol. 10, 1724–1736. https://doi.org/10.1111/j.1365-2486.2004.00826.x.

Zhang, J., Gou, X., Alexander, M.R., Xia, J., Wang, F., Zhang, F., Man, Z., Pederson, N., 2021. Drought limits wood production of Juniperus przewalskii even as growing seasons lengthens in a cold and arid environment. Catena 196, 104936. https://doi.org/10.1016/j.catena.2020.104936.

Zhang, J., Gou, X., Pederson, N., Zhang, F., Niu, H., Zhao, S., Wang, F., 2018. Cambial phenology in Juniperus przewalskii along different altitudinal gradients in a cold and arid region. Tree Physiol. 38, 840–852. https://doi.org/10.1093/treephys/tpx160.

Zhang, Y., Wilmking, M., 2010. Divergent growth responses and increasing temperature limitation of Qinghai spruce growth along an elevation gradient at the northeast Tibet Plateau. Forest Ecol. Manag. 260, 1076–1082. https://doi.org/10.1016/j.foreco.2010.06.034.